

The Role of Motion Dynamics in the Design, Control and Stability of Bipedal and Quadrupedal Robots

Michael Hardt and Oskar von Stryk

Department of Computer Science, Technische Universität Darmstadt
Alexanderstr. 10, 64283 Darmstadt, Germany

{hardt,stryk}@sim.tu-darmstadt.de

www.sim.informatik.tu-darmstadt.de

Abstract. Fundamental principles and recent methods for investigating the nonlinear dynamics of legged robot motions with respect to control, stability and design are discussed. One of them is the still challenging problem of producing dynamically stable gaits. The generation of fast walking or running motions require methods and algorithms adept at handling the nonlinear dynamical effects and stability issues which arise. Reduced, recursive multibody algorithms, a numerical optimal control package, and new stability and energy performance indices are presented which are well-suited for this purpose. Difficulties and open problems are discussed along with numerical investigations into the proposed gait generation scheme. Our analysis considers both biped and quadrupedal gaits with particular reference to the problems arising in soccer-playing tasks encountered at the RoboCup where our team, the Darmstadt Dribbling Dackels, participates as part of the German Team in the Sony Legged Robot League.

1 Introduction

RoboCup and Dynamics of Legged Robot Motion. The RoboCup scenario of soccer playing legged robots represents an extraordinary challenge for the design, control and stability of bipedal and quadrupedal robots. In a game, fast motions are desired which preserve the robot's stability and can be adapted in real-time to the quickly changing environment. Existing design and control strategies for bipedal and quadrupedal robots can only meet these challenges to a small extent.

During the nineties, both trajectory planning methods relying on nonlinear robot dynamics and model-based control methods have evolved into the state-of-the-art for developing and implementing fast and accurate motions for industrial manipulators. Successful control of the nonlinear robot dynamics is also the key to fast and stable motions of bipedal and quadrupedal robots. Many subproblems remain unsolved in fulfilling this objective. This paper contributes to this ambitious goal by discussing fundamental principles and recent methods in the modeling, simulation, optimization and control of legged robot dynamics.

Nonlinear Dynamics of Legged Robot Motion. A precise modeling of fast moving legged locomotion systems requires high dimensional nonlinear multi-body dynamics which can accurately describe the nonlinear relationships existing between all linear and rotational forces acting at each joint and the feet on the one hand and the position, velocity and acceleration of each link in the kinematic tree-structure on the other hand. It is thus a complex task to generate and control stable motions for such systems. Biped and quadruped constructions generally consist of a minimum of five bodies with two to six degrees of freedom (DoF) per leg in addition to the six DoF corresponding to the base body in order to give the necessary amount of motion dexterity necessary for a wide range of movement. Dynamic model simplifications in previous work, however, have generally ranged from pendulum models [22] to multi-link planar models [5,6,14,16] for bipeds and for quadrupeds [17] or to multi-link spatial models [20,27]. Though these simplifications allow one to analyze certain predominant behaviors of the dynamic system, many other important features are lost. A complete and complex dynamical system description will contain much more of the significant dynamical effects, yet a control solution for these models based on an analytical approach is usually not possible and results must be sought for numerically.

The dynamic effects characterizing bipedal and quadrupedal motion may be further complicated by external disturbance factors and forces, quickly changing system goals, low friction conditions, a limited power source, and inexact sensor information resulting from fast movements and a highly dynamic environment. These are all characteristics of the difficulties encountered in the Four-Legged and Humanoid Leagues of the RoboCup soccer challenge.

Solutions for Multibody Dynamics of Legged Robot Models. Multibody dynamical models for real legged systems are typically characterized by a high number of DoF, relatively few contact constraints or collision events, and a variety of potential ground contact models, actuator models, and mass-inertial parameter settings due to changing load conditions. Such detailed multibody dynamical models are generally required for the realistic reproduction of legged system behavior in gait optimization (Sect. 4.2), tuning of construction design parameters (Sect. 6), or in simulation and feedback control (Sect. 5). Closed-form dynamical expressions are the most efficient form of evaluating the dynamics, but are not well-suited to legged systems due to the many changing kinematic and kinetic parameters. Recursive, numerical algorithms are also highly efficient for large systems and permit the easy interchangeability of parameters and the introduction of external forces without repeated extensive preprocessing (Sect. 2.2). This approach has been used here. Reduced dynamical approaches appropriate for legged robots are additionally presented in Sect. 2.2.

Dynamical Stability of Legged Robot Motion. There exists a wide spectrum of previously presented approaches for generating dynamically stable motions in bipeds and quadrupeds. Analytical methods [14,19,22] usually rely on simplified models and are not yet at a stage where the many influencing dynamical effects previously mentioned can be considered. More complete 3-D modeling

approaches [20,27] for bipeds generally rely on heuristic schemes to construct dynamically stable motions. The dynamic stability criterion is usually based on the Zero-Moment-Point [35] yet this criterion is limited in its ability to classify stability [12] during, for example, periods of rolling motion of the feet, which for fast-moving systems can be considerable. In the case of quadrupeds with point contacts, a similar problem occurs. Such gait planning techniques also rarely consider the stabilizing potential of the torso sway motion or that of arm swinging which can be advantageous for increasing robustness and reducing power consumption. Nonetheless, 3-D bipeds and quadrupeds have been constructed which perform dynamically stable walking and running [18,34,37]. Though due to excessive power consumption they were either not autonomous or required a substantial battery supply for only a short operational period. In Sect. 3, alternative stability as well as energy-based performance measures suited for bipedal and quadrupedal gait generation are presented.

Numerical Optimization and Feedback Control of Bipedal and Quadrupedal Robot Motions. Algebraic control strategies for legged systems cannot yet handle the high dimension and many modeling constraints present in the locomotion problem. Heuristic control methods, on the other hand, tend to have poor performance with respect to power efficiency and stability and require much hand-tuning to acquire an acceptable implementation in a fast-moving legged system. The remaining proven approach is the use of sophisticated numerical optimization schemes to generate optimal trajectories subject to the numerous modeling constraints. The resulting trajectories may later be tracked or used to approximate a feedback controller in the portion of state space of interest.

In our efforts to achieve dynamically stable and efficient gaits for the Sony RoboCup quadruped (Figure 1) and our own competition biped currently under construction, we explore in this work a numerical optimization approach which minimize performance or stability objectives in the gait generation problem. Numerical optimization tools have advanced sufficiently [2,11,32] such that all the above-mentioned modeling and stability constraints can be incorporated into the problem formulation together with a relatively complete dynamical model so as to obtain truly realistic energy-efficient, stable and fast motions. The optimization approach described in Sect. 4.1 has been developed during the last decade and has already been successfully applied for gait planning in bipeds in two dimensions [16] and for quadrupeds [17].

2 Dynamic Modeling of Legged Locomotion

2.1 Two Case Studies for Biped and Quadruped Dynamics

Two models of a bipedal and a quadrupedal robot are treated here. The presented approach, however, is applicable to any other legged robot design.

Our model for the Sony quadruped (see Fig. 1) consists of a 9-link tree-structured multibody system with a central torso attached to a relatively heavy head at a fixed position and four two-link legs. Each leg contains a 2 DoF universal joint in the hip and a 1 DoF rotational joint in the knee. A (almost) minimum

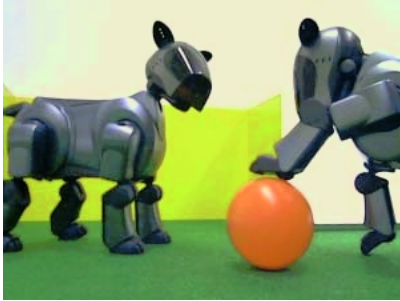


Fig. 1. Four-legged Sony robots

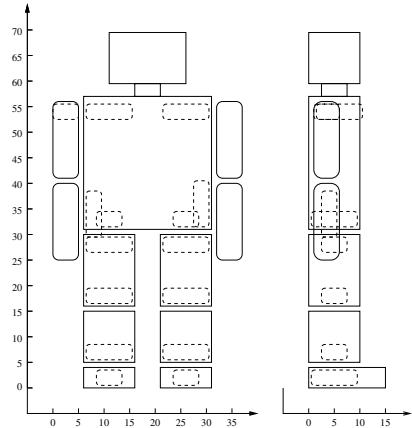


Fig. 2. Design of humanoid robot prototype

set of coordinates consists of 19 position and 19 velocity states ($\mathbf{q}(t), \dot{\mathbf{q}}(t)$) which include a four-parameter unit quaternion vector for the orientation, a three-dimensional global position vector, and their time derivatives for the torso, and additionally three angles and their velocities for each leg. The 12 control variables $\mathbf{u}(t)$ correspond to the applied torques in the legs. The required kinematic and kinetic data for each link (length, mass, center of mass, moments of inertia) have been provided by Sony. A refined model will be used in further investigations which also includes the three motion DoF for the head.

The physical dimensions for our biped prototype fall under the specifications set for the 80 *cm* category of the RoboCup competition¹. The biped (Fig. 2) has six DoF (hip 3, knee, 1, foot 2) in each leg and 2 DoF in the shoulder so that a coordinate set consists of 23 position and 23 velocity states ($\mathbf{q}(t), \dot{\mathbf{q}}(t)$) including 7 position states with a quaternion and position vector to describe the torso orientation and position. There are 16 actuated joints whose input torques are represented in the control vector $\mathbf{u}(t)$. Different to quadruped gaits where in many cases a foot contact model may be sufficient, a foot contact area must be considered for a biped.

In both cases, the structure of the equations of motion are those for a rigid, multibody system experiencing contact forces,

$$\begin{aligned} \ddot{\mathbf{q}} &= \mathcal{M}(\mathbf{q})^{-1} \left(B\mathbf{u} - \mathcal{C}(\mathbf{q}, \dot{\mathbf{q}}) - \mathcal{G}(\mathbf{q}) + J_c(\mathbf{q})^T \mathbf{f}_c \right) \\ 0 &= \mathbf{g}_c(\mathbf{q}) , \end{aligned} \quad (1)$$

where N equals the number of links, $\mathcal{M} \in \mathbb{R}^{N \times N}$ is the positive-definite mass-inertia matrix, $\mathcal{C} \in \mathbb{R}^N$ contains the Coriolis and centrifugal forces, $\mathcal{G} \in \mathbb{R}^N$ the gravitational forces, and $\mathbf{u}(t) \in \mathbb{R}^m$ are the control input functions which are

¹ http://www.robocup.org/regulations/humanoid/rule_humanoid.htm

mapped with the constant matrix $B \in \mathbb{R}^{N \times m}$ to the actively controlled joints. The ground contact constraints $\mathbf{g}_c \in \mathbb{R}^{n_c}$ represent holonomic constraints on the system from which the constraint Jacobian may be obtained $J_c = \frac{\partial \mathbf{g}_c}{\partial \mathbf{q}} \in \mathbb{R}^{n_c \times N}$, while $\mathbf{f}_c \in \mathbb{R}^{n_c}$ is the ground constraint force.

2.2 Robotic Dynamic Algorithms

Many methods exist for evaluating multibody robot dynamics. Symbolic methods construct efficient, closed form dynamics for the *specific* multibody systems through symbolic simplifications [28]. This approach is not well-suited though to legged systems due to the switching characteristic of the dynamics in different contact states, varying parameter and exterior load conditions. The Composite Rigid Body Algorithm (CRBA) [36] numerically solves the equations of motion efficiently by first assembling the entire mass matrix \mathcal{M} and then solving the resulting system. It is used in many commercial packages, and it permits an easy change of parameters or the introduction of additional external forces directly. These solution methods are, in general, superseded in modularity and in efficiency for systems with more than 7–8 links by the articulated body algorithm (ABA) of $\mathcal{O}(N)$ complexity [9].

The ABA [8,31] is a very exact and numerically stable multibody algorithm superior to the CRBA as it introduces less cancellations [29]. It exploits the linear relationship between accelerations and applied forces in a rigid-body system. The definition of the articulated body inertia, the inertia of the ‘floppy’ outboard chain of rigid bodies not subject to applied forces, permitted the construction of a recursive forward dynamics algorithm [8]. Similarities to the Kalman filtering algorithm then led to an alternative decomposition of the mass-inertia matrix and, consequently, to an $\mathcal{O}(N)$ recursive algorithm for calculating the inverse mass matrix \mathcal{M}^{-1} [31]. A description of the original algorithms may be found in [8,31] with improvements found in [15,25,29].

For numerical reasons, it is often convenient to work with a dynamical system free of contact constraints. Many standard discretization or integration schemes found in optimization or simulation software can then be applied. It is generally possible to convert the contact dynamics in legged systems into a reduced-dimensional, unconstrained equation by projecting (1) onto a set of independent states. The resulting ODE can be evaluated efficiently using a recursive multibody algorithm [16]. The approach requires solving the inverse kinematics problem for the dependent states. A closed-form solution exists for common leg constructions with knowledge of the relative hip and foot contact locations by defining the contact leg states as the dependent states.

The position state vector \mathbf{q} may be partitioned into independent position states \mathbf{q}_1 and dependent position states \mathbf{q}_2 obtained from \mathbf{q} via a linear transformation, $\mathbf{q}_1 = Z\mathbf{q}$. The transformation $Z \in \mathbb{R}^{(N-n_c) \times N}$ is in the case of legged systems a constant full-rank matrix consisting of unit vectors or $\mathbf{0}$. The dependent position states \mathbf{q}_2 are calculated from \mathbf{q}_1 with the inverse kinematics function $i(\cdot)$, $\mathbf{q}_2 = i(\mathbf{q}_1)$, which for legged systems can generally be expressed in closed-form [15]. One may partition the constraint velocity equation

$J_c \dot{\mathbf{q}} = 0$ with respect to the independent $\dot{\mathbf{q}}_1$ and dependent velocity states $\dot{\mathbf{q}}_2$, $J_{c,1} \dot{\mathbf{q}}_1 + J_{c,2} \dot{\mathbf{q}}_2 = 0$. This similarly provides a change of variables for the velocity states,

$$\dot{\mathbf{q}}_1 = Z \dot{\mathbf{q}}, \quad \dot{\mathbf{q}}_2 = -J_{c,2}^{-1} J_{c,1} \dot{\mathbf{q}}_1 . \tag{2}$$

Substituting \mathbf{q}_1 , \mathbf{q}_2 , $\dot{\mathbf{q}}_1$, and $\dot{\mathbf{q}}_2$ into (1) and multiplying (1) by Z then gives an ODE of size $(N - n_c)$

$$\ddot{\mathbf{q}}_1 = Z \mathcal{M}(\mathbf{q}_1, i(\mathbf{q}_1))^{-1} \times \left(B \mathbf{u} - \mathcal{C}(\mathbf{q}_1, i(\mathbf{q}_1), \dot{\mathbf{q}}_1, -J_{c,2}^{-1} J_{c,1} \dot{\mathbf{q}}_1) - \mathcal{G}(\mathbf{q}_1, i(\mathbf{q}_1)) + J_c^T \mathbf{f}_c \right). \tag{3}$$

The principal advantage of this approach is that one need only perform the optimization on the reduced dimensional state. The state must then be monitored such that it remain within a well-defined region of the state space. In Sect. 4.2, where the optimal amble gait is investigated for a quadruped, there are always two legs in contact. As a result, instead of the full 36 states $(\mathbf{q}, \dot{\mathbf{q}})$, 24 states can describe the system.

2.3 Constraints

An important aspect of formulating a gait optimization problem is establishing the many constraints on the problem. Legged systems are examples of general hybrid dynamical systems [17] as they periodically enter different discrete states with each new contact state which (discontinuously) switch the dynamical model. The numerical solution of hybrid optimal control problems is in its early stages [3,33], yet when the discrete trajectory (contact events) is previously specified, current numerical solution techniques have been shown to work well [5,16].

Specifying the order of contact events for a biped is easy as one need only distinguish between walking and running. The range of different quadruped gaits, however, can be quite large. The problem of searching over all possible gaits in a gait optimization problem has not yet been completely solved [17]. Biological studies, however, can provide a good indication as to which quadrupedal gaits are the most efficient at different speeds [1]. A numerical advantage for considering gaits with the left and right legs of a pair with equal duty factors is that the problem can be completely formulated within half a gait cycle. This is not a severe restriction as both symmetric and asymmetric gaits fit within this framework; the relative phases of each leg are free.

Summary of the modeling constraints for a *complete* gait cycle in $[0, t_f]$:

Periodic gait constraints (enforced during gait optimization):

1. Periodicity of continuous state and control variables: $\mathbf{q}(t_f) = \mathbf{q}(0)$, $\dot{\mathbf{q}}(t_f^+) = \dot{\mathbf{q}}(0)$, where $\dot{\mathbf{q}}(t_f^+) := \lim_{\epsilon > 0, \epsilon \rightarrow 0} \dot{\mathbf{q}}(t_f + \epsilon)$.
2. Periodicity of ground contact forces: $\mathbf{f}_c(t_f^+) = \mathbf{f}_c(0)$.

Exterior environmental constraints:

1. Kinematic constraints on the height (z -coordinate) of the swing leg tips. The leg tip height $q_{tip,z}$ is calculated from a forward kinematics function $FK(\cdot)$ of the position states \mathbf{q} :

$$q_{tip,z} = FK(\mathbf{q}(t)) \geq 0. \quad (4)$$

In the case of unlevel ground, the 0 may be replaced by a ground height function of the horizontal position of the swing leg tips. We consider here only level ground.

2. Ground contact forces lie within the friction cone and unilateral contact constraints are not violated [10,30]. In the case of point contact, ground linear contact forces $\mathbf{F} = [F_x \ F_y \ F_z]^T$ must satisfy (otherwise a slipping contact state is entered)

$$\sqrt{F_x^2 + F_y^2} \leq \mu_t F_z, \quad F_z \geq 0 \quad (5)$$

with friction coefficient μ_t . The contact force vector \mathbf{f}_c which appears in (1) is composed of all the contact linear force vectors $\{\mathbf{F}_j\}$ from each contact leg j .

In the case of multiple contact, such as a foot lying flat on the ground, the rotational contact force vector $\mathbf{T}_j = [T_{j,x} \ T_{j,y} \ T_{j,z}]^T$ is additionally constrained

$$|T_x| \leq 0.5F_z l_y, \quad |T_y| \leq 0.5F_z l_x, \quad |T_z| \leq \mu_d F_z \quad (6)$$

where μ_d is a friction coefficient, and l_x and l_y are the length and width of the foot.

Interior modeling constraints:

1. Jump conditions in the system velocities due to inelastic collisions of the legs with the ground. If the exterior constraint (4) is violated, a collision occurs. The resulting instantaneous jump in the state velocities at the k -th such collision event is

$$\dot{\mathbf{q}}(t_{S,k}^+) = \text{Jump}_{q,q'}(\mathbf{q}(t_{S,k}^-), \dot{\mathbf{q}}(t_{S,k}^-)) \quad (7)$$

where $\mathbf{q}(t_{S,k}^-)$ and $\dot{\mathbf{q}}(t_{S,k}^+)$ indicate the values of \mathbf{q} just before and after the collision event respectively. The function Jump calculates the jump in the state velocities resulting from the point of collision instantaneously reaching a zero velocity. The jump is physically modeled as the consequence of an impulsive force propagating throughout the system which may be calculated using the law of conservation of angular momentum. This form is an approximation to real collision phenomena and is better tractable numerically than using mixed elastic-inelastic collision models.

2. Magnitude constraints on states, controls and control rates:

$$L_{\mathbf{q}} \leq \mathbf{q} \leq U_{\mathbf{q}}, \quad L_{\dot{\mathbf{q}}} \leq \dot{\mathbf{q}} \leq U_{\dot{\mathbf{q}}}, \quad L_{\mathbf{u}} \leq \mathbf{u} \leq U_{\mathbf{u}}, \quad L_{\dot{\mathbf{u}}} \leq \dot{\mathbf{u}} \leq U_{\dot{\mathbf{u}}} \quad .$$

$L_{(\cdot)}$ and $U_{(\cdot)}$ are constant vectors of length equal to their arguments.

3. Actuator torque-speed limitations. The applied torque at the actuated joint i is constrained by the characteristic line of the motor-gear train: $|u_i| \leq (\dot{\theta}_{max,i} - |\dot{\theta}_i|) \frac{G_i^2 \eta_i}{m_i}$, where u_i is the applied torque at joint i , $\dot{\theta}_i$ and $\dot{\theta}_{max,i}$ are the joint i velocity and maximum absolute joint velocity respectively, G_i is the gear ratio, η_i is the gear efficiency, and m_i is the slope of the motor characteristic line.

Numerical simulation of legged locomotion must not only enforce the interior constraints and robot dynamics but must also supervise the environmental constraints. When the latter can no longer be enforced, the system enters a new discrete state often leading to a switch in the system's state and dynamics, which in turn must reflect the interior modeling constraints.

3 Dynamic Stability and Performance

3.1 Measures of Stability

There exists a general agreement on the definition of static stability for legged systems: the ground projection of the center of mass (GCoM) lies within the convex hull of its foot-support area. Various forms of static stability margins have been defined usually concerning the minimum distance between the GCoM and the support boundary which have served to develop statically stable walking motions in all types of legged systems. There exists, however, no general consensus on a mathematical description for dynamic stability other than "its negation implies a lack of static stability and an unsustainable gait" [12]. In [19], dynamic stability was categorized into postural stability and gait stability. Postural stability is maintained when the posture (torso orientation and position) remains within a bounded range of values. Gait stability refers to the dynamical system definition of stability for limit cycles in periodic gaits. Numerical methods for classifying or acquiring stable gait trajectories are presented in [21] and [26] respectively. Due to the nonconvexity of the problem and the high dimensional nonlinear dynamics, direct optimization methods cannot be readily applied to the full-dimensional dynamical model and, thus, we do not consider this problem here.

The zero-moment-point (ZMP) and its relationship with the support polygon is often used for measuring postural stability [18,19,20,27,35]. The ZMP is that point on the ground where the total moment generated due to gravity and inertia equals zero or equivalently the point where the net vertical ground reaction force acts. As pointed out in [12], this point cannot leave the support polygon and, in the case when the foot is rotating about a point, it lies directly on the edge of the support polygon. That is during periods of single foot support in biped walking when the foot is rotating about the heel or the toe, the ZMP does not provide information as to the amount of instability in the system. This period can amount

to up to 80% of a normal human walking gait. Evidently, fast dynamically stable biped walking and running requires foot rotation for stability and efficiency. The alternative measure proposed in [12], the foot-rotation-indicator (FRI), coincides with the ZMP during periods of static equilibrium of the foot and otherwise provides information as to the foot's rotational instability. Foot rotation instability measured by the FRI is a more complete measure of postural instability, but it still does not provide any information as to gait stability/instability.

Within all possible quadrupedal gaits [1] (pace, gallop, amble, etc.), there exist many configurations where the ZMP provides little useful information. The FRI can also be extended to the quadrupedal case though other similar measures specialized to quadrupeds have been introduced. In [24], the angular momentum about the support edges was used to define a postural stability index. Like the FRI, this method provides both directional information and a reference stability quantity that can be used to quantify system instability. Though postural stability measures are not rigorous dynamical system stability measures, these measures provide a means to monitor the stability or instability present in legged systems. Another advantage is that these measures may be directly incorporated into controllers for *on-line* use and, additionally, they can treat aperiodic gaits, a necessity in an environment containing obstacles.

3.2 Performance Specifications

The minimization of several, alternative performance functions measuring (in-)stability and/or efficiency of the periodic motion enables (at least locally) optimal and unique trajectories for the states \mathbf{q} , $\dot{\mathbf{q}}$ and controls \mathbf{u} .

Stability Performance 1: The FRI point may be computed as that point \mathbf{S} for which the net ground tangential impressed forces (FI_x, FI_y) acting on the foot are zero. These forces are the acting forces and may differ from the constraint forces $\mathbf{F} = [F_x \ F_y \ F_z]^T$ [12]. If N_f feet/leg-tips are in contact with the ground, \mathbf{S} may be considered as the net point of action for all ground impressed forces resulting from the robot gravity and inertial forces. It may be computed using the rotational static equilibrium equation for the feet,

$$\sum_{j=1}^{N_f} \left(\mathbf{n}_j + \mathbf{S}\mathbf{O}_j \times \mathbf{f}_j - \mathbf{S}\mathbf{G}_j \times m_j \mathbf{g} \right)_T = 0, \quad (8)$$

where \mathbf{n}_j and \mathbf{f}_j are the moment and linear force vectors from contact foot j acting on its connecting point \mathbf{O}_j to the remainder of the robot, $\mathbf{S}\mathbf{O}_j$ and $\mathbf{S}\mathbf{G}_j$ are the vectors from \mathbf{S} to \mathbf{O}_j and the foot center of mass \mathbf{G}_j respectively, m_j is the foot mass, and \mathbf{g} is the gravity vector. The subscript T indicates that only the ground tangential x- and y-coordinates must satisfy the equation. A stability performance index which may be used for maximizing postural stability is the average distance in the ground plane between the point \mathbf{P} and the ground projected center of mass \mathbf{GCoM} .

$$\mathbf{J}_{s1}[\mathbf{q}, \dot{\mathbf{q}}, \mathbf{u}] = \int_0^{t_f} ((\mathbf{GCoM}_x - S_x)^2 + (\mathbf{GCoM}_y - S_y)^2) dt \quad (9)$$

Stability Performance 2: The measure proposed in [24] is an alternative measure based on the angular momentum and it takes into consideration the momentum of the swing legs. It is however limited to gaits with at least two legs in contact with the ground. The stability/instability margin is equal to:

$$S_H(t) = \min\{S_H^l(t), l = 1, \dots, n_l\}, \quad t \in [0, t_f], \quad (10)$$

where n_l is the number of edges in the support polygon. The stability values S_H^l for each edge depend on whether the edge is a diagonal or non-diagonal edge.

In the case of a non-diagonal support edge, $S_H^l = H_l^{\text{ref}} - H_l$ where the reference angular momentum H_l^{ref} about edge l is defined as the minimum angular momentum to tip over the edge if the system were an inverted pendulum $H_l^{\text{ref}} = (\mathbf{r}_{l,CM} \times m_{\text{total}} \mathbf{v}_{\text{ref}}) \cdot \hat{\mathbf{e}}_l$ and H_l is the rotational tendency about that edge $H_l = \mathbf{H}_P \cdot \hat{\mathbf{e}}_l$. Here, $\mathbf{r}_{l,CM}$ is the orthogonal vector from edge l to the system center of mass \mathbf{CoM} , m_{total} is the total system mass, \mathbf{v}_{ref} is the reference velocity vector computed from the kinetic energy required to attain the higher potential energy at which the system \mathbf{CoM} would lie above edge l , \mathbf{H}_P is the angular momentum about a point P on the support edge, and $\hat{\mathbf{e}}_l$ is a unit vector along the edge.

In the case of a diagonal support edge, $S_H^l = \{\min(H_l - H_l^{\text{ref}}, H_l^{\text{max}} - H_l) : \text{two legs in contact \& GCoM before diagonal edge}, S_H^l = H_l^{\text{max}} - H_l : \text{two legs in contact \& GCoM past diagonal edge}, S_H^l = H_l^{\text{max}} - H_l : \text{third support leg behind diagonal support edge}, S_H^l = H_l^{\text{ref}} - H_l : \text{third support leg in front of diagonal support edge}\}$, where the maximum angular momentum about $\hat{\mathbf{e}}_l$ is defined as $H_l^{\text{max}} = (\mathbf{r}_{l,CM} \times m_{\text{total}} \mathbf{v}_{\text{tip}}^{\text{max}}) \cdot \hat{\mathbf{e}}_l$ and $\mathbf{v}_{\text{tip}}^{\text{max}}$ is the maximum velocity vector of the swing leg's tip.

A worst-case stability measure is defined as the minimum value of S_H over the entire gait cycle which should be maximized to find the best worst-case performance. Introducing an additional control parameter p_1 , the min-max objective may be transformed to a standard Mayer-type, $p_1 := \min_{0 \leq t \leq t_f} S_H(t)$, where an additional inequality constraint is needed, $S_H(t) - p_1 \geq 0$ ($0 \leq t \leq t_f$), and the performance index becomes

$$\mathbf{J}_{s2}[\mathbf{p}] = -p_1. \quad (11)$$

Energy Performance 1: In the case of robots where a high torque is generated by a large current in the motor, the primary form of energy loss is called the Joule thermal loss [23]. Define R_i , G_i , and K_i as the armature resistance, gear ratio, and torque factor for link i respectively. Also let d_S be the forward distance traveled during one gait cycle, then the normalized average energy loss to be minimized is

$$\mathbf{J}_{e1}[\mathbf{u}] = \frac{1}{d_S} \int_0^{t_f} \sum_{i=1}^N R_i \left(\frac{u_i}{G_i K_i} \right)^2 dt. \quad (12)$$

Energy Performance 2: In [13], the specific resistance ϵ was used to measure efficiency or more precisely an average power consumption normalized over distance traveled. It is a dimensionless quantity, and by minimizing its integral over the gait cycle, a normalized form of the kinetic energy is minimized. Let

mg be the system weight of the system, $\dot{\theta}_i(t)$ is the joint i angle velocity contained within the velocity state vector $\dot{\mathbf{q}}(t)$, and $v(t)$ is the forward velocity. The performance index to be minimized is

$$\mathbf{J}_{e2}[\mathbf{q}, \dot{\mathbf{q}}, \mathbf{u}] = \int_0^{t_f} \frac{\sum_{i=1}^N |u_i \dot{\theta}_i|}{mgv} . \tag{13}$$

Summary: Stability performance 1 delivers a solution with a minimum average level of postural instability during the gait while stability measure 2 is intended towards improving the worst-case unstable configuration occurring in a gait. Energy performance 1 is a direct measure of energy loss in the joints normalized over the distance traveled, and energy performance 2 measures average power consumption.

4 Trajectory Optimization and Numerical Investigations

The optimization of the stability or energy performance functions of Sect. 3.2 with respect to the controls $\mathbf{u}(t)$ over a period of time $[0, t_f]$ and subject to the system dynamics and constraints of Sect. 2 leads to optimal control problems. Although the computation of the optimal, state feedback control is the ultimate goal where the control is a function of the system state vector \mathbf{x} , $\mathbf{u}^*(\mathbf{x})$, it cannot be computed directly because of the system’s high dimension, nonlinearity and constraints. However, with the help of numerical optimization methods developed during the last decade, optimal open loop trajectories $\mathbf{x}^*(t)$, $\mathbf{u}^*(t)$, $0 \leq t \leq t_f$, can nowadays be computed efficiently [2,32].

4.1 Trajectory Optimization Framework

The optimization we are faced with is to find the unknown open-loop state and control trajectories $(\mathbf{x}(t), \mathbf{u}(t))$ which minimize a performance function \mathbf{J} (Sect. 3.2) subject to a set of possibly switching differential equations f^k (resulting from the legged robot dynamics of Sects. 2.1–2.3, i.e., $\mathbf{x} = (\mathbf{q}, \dot{\mathbf{q}})$), nonlinear inequality g_i^k and equality h_i^k constraints, and boundary conditions r_i^k (resulting from the constraints and conditions of Sect. 2.3). All constraints of the dynamic optimization problem are formulated in the general first order form

$$\dot{\mathbf{x}}(t) = \begin{cases} f^1(\mathbf{x}(t), \mathbf{u}(t), \mathbf{d}(t), \mathbf{p}, t), & t \in [0, t_{S,1}], \\ f^k(\mathbf{x}(t), \mathbf{u}(t), \mathbf{d}(t), \mathbf{p}, t), & t \in [t_{S,k-1}, t_{S,k}], \quad k = 2, \dots, m-1 \\ f^m(\mathbf{x}(t), \mathbf{u}(t), \mathbf{d}(t), \mathbf{p}, t), & t \in [t_{S,m-1}, t_f], \end{cases}$$

$$\begin{aligned} g_i^k(\mathbf{x}(t), \mathbf{u}(t), \mathbf{d}(t), \mathbf{p}, t) &\geq 0, \quad t \in [t_{S,k-1}, t_{S,k}], \quad i = 1, \dots, n_{g_m^k}, \quad k = 1, \dots, m, \\ h_i^k(\mathbf{x}(t), \mathbf{u}(t), \mathbf{d}(t), \mathbf{p}, t) &= 0, \quad t \in [t_{S,k-1}, t_{S,k}], \quad i = 1, \dots, n_{h_m^k}, \quad k = 1, \dots, m, \end{aligned}$$

$$\begin{aligned} r_i^1(\mathbf{x}(0), \mathbf{u}(0), \mathbf{d}_0, \mathbf{p}, 0, \mathbf{x}(t_f), \mathbf{u}(t_f), \mathbf{d}_f, t_f) &= 0, \quad i = 1, \dots, r_m^k, \\ r_i^k(\mathbf{x}(t_{S,k}^-), \mathbf{u}(t_{S,k}^-), \mathbf{d}(t_{S,k}^-), \mathbf{p}, t_{S,k}, \mathbf{x}(t_{S,k}^+), \mathbf{u}(t_{S,k}^+), \mathbf{d}(t_{S,k}^+)) &= 0, \quad k = 2, \dots, m-1. \end{aligned}$$

The integer-valued discrete state trajectory $\mathbf{d}(t)$ is assumed to be constant in each phase $[t_{S,j-1}, t_{S,j}]$ and describes the sequence of switches of the system dynamics, i.e., a quadrupedal gait, and must generally be provided. The program DIRCOL [32] uses the method of sparse direct collocation to approximate the piecewise continuous states \mathbf{x} , controls \mathbf{u} , and constant parameters \mathbf{p} of the optimal control problem. This leads to a multiphase optimal control problem to be solved in all phases $[t_{S,j-1}, t_{S,j}]$ through adaptively selected grids $t_{S,j-1} = t_1^j < t_2^j < \dots < t_{n_G,j}^j = t_{S,j}$ in each subinterval $t \in [t_k^j, t_{k+1}^j]$ by the approximation

$$\begin{aligned} \hat{\mathbf{u}}_{app}(t) &= \beta(\hat{\mathbf{u}}(t_k^j), \hat{\mathbf{u}}(t_{k+1}^j)), & \beta - \text{linear} \\ \hat{\mathbf{x}}_{app}(t) &= \alpha(\hat{\mathbf{x}}(t_k^j), \hat{\mathbf{x}}(t_{k+1}^j), f_k^j, f_{k+1}^j), & \alpha - \text{cubic} \end{aligned} \quad (14)$$

where $f_k^j = f^j(\hat{\mathbf{x}}(t_k^j), \hat{\mathbf{u}}(t_k^j), \mathbf{p}, t_k^j)$ [32]. The infinite-dimensional optimal control problem is thereby converted to a finite dimensional, but large-scale and sparse, nonlinearly constrained optimization problem containing the unknown values for \mathbf{x} , \mathbf{u} at the discretization grid as well as \mathbf{p} , $t_{S,i}$, t_f . The problem is then solved using an SQP method for sparse systems SNOPT [11]. The resulting optimal control method is thus equipped to handle the complexities of the walking problem: unknown liftoff times $t_{S,i}$, different ground contact combinations for the legs $\mathbf{d}(t)$, discontinuous states at collision times $t_{S,k}$ of the legs with the ground, switching dynamics, and actuation limits.

This method of generating optimal reference trajectories was also used in [7,16,17]. It may be applied to much higher dimensional systems than finite-element approaches as used for example in [4], and the numerical package is more general than that for example used in [5].

4.2 Numerical Investigations for the Quadruped

The goal in our numerical investigations is to plan and implement efficient, stable, and rapid periodic motions for our test platforms of the Sony four-legged robot and our humanoid robot currently under construction (Sect. 6). To obtain starting values when setting up the iterative optimization procedure from scratch, a series of optimal solutions for subproblems was computed. First the problem was solved in two dimensions with most parameters fixed, then all constraints were gradually relaxed using the previous solution to start the subsequent problem. Optimization run times for a single subproblem ranged from 5 to 20 minutes on a Pentium III, 900 MHz PC.

In our investigations, dynamically stable quadruped gaits were investigated with *Stability Performance 2*. Energy efficiency is not as important for the quadruped in RoboCup competition (Fig. 1) since the robot's battery provides sufficient power for the duration of half a regulation match. An optimization over this min-max performance will optimize the worst-case configuration, thereby facilitating a more robust closed-loop implementation.

The solution displayed in Fig. 3 is for a desired forward velocity of 40 *m/min* or 0.67 *m/s*. The optimal gait stride is 0.416 *m* and the gait period is 1.25

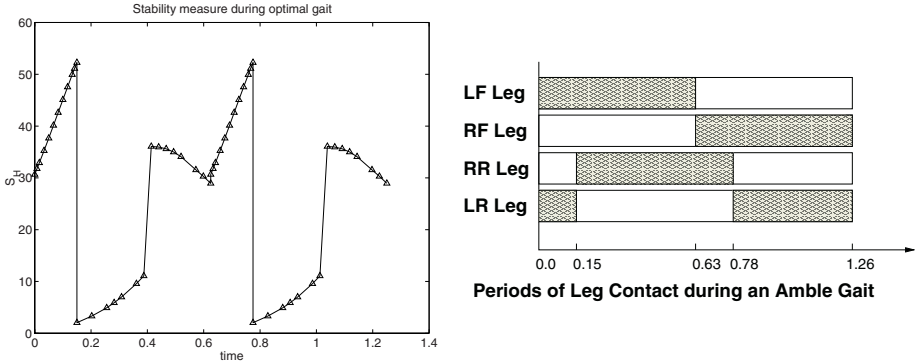


Fig. 3. Stability index S_H for an optimized amble gait of a quadruped moving forward at 0.67 m/s and duty factor $\beta = 0.5$ based on a full, spatial dynamical model. The first sharp drop in the stability index occurs at the instant when the RR (right rear) leg initially makes contact and the (left rear) leg breaks contact. At that time the diagonally opposed legs support the body and a minimally sufficient amount of forward momentum exists to bring the system **CoG** over the support edge. As the **CoG** approaches the support edge, the stability index increases then falls again once this point has been passed. The second half of the gait is symmetric to the first half

seconds. Fig. 3 shows the evolution of the optimized stability index S_H over one gait period. A negative value of S_H indicates an unstable configuration while the more positive S_H is, the more stable the system. The large variations in the index are caused by the changing of support legs in the robot. The gait displayed is an amble gait between walking and running with the legs having a duty factor of $\beta = 0.5$ which is a demanding, fast-moving gait. The order of support leg order is (LF-LB, LR-RR, RF-RR, RF-LR: LF=left front, RR=right rear) so that the system alternates between having two support legs on one side and diagonal support legs. The steepest drop in S_H occurs when the system switches from a side pair of support legs to a diagonal pair. At that point the angular momentum of the system about the diagonal edge is slightly greater than the required angular momentum for the **CoM** to “roll over” the diagonal edge and not fall backward. A conservative value of 2 m/sec was chosen for the attainable velocity of the swing leg tip \mathbf{v}_{tip}^{max} .

Our investigations are continuing with a thorough investigation and comparison of the stability/energy performances and their combinations as presented in Section 3.2. Furthermore, they will be evaluated using gait stability tools, tested with a real-time legged system simulator currently under development in our group. At RoboCup 2002 we plan to present optimized motion primitives implemented on the actual quadruped using trajectory-following controllers.

5 Control of Bipedal and Quadrupedal Robot Motions

Today, most all feedback walking control strategies that have been implemented successfully in three-dimensional humanoid robots or quadrupeds are based on

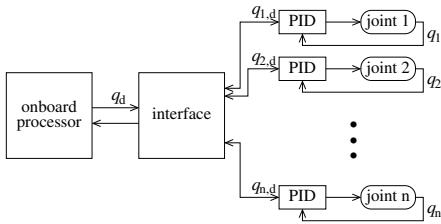


Fig. 4. Structure of a decentralized trajectory tracking control scheme: The local feedback control loops operate within milliseconds and are implemented using a microprocessor for each joint. The reference trajectories are provided or generated by an onboard processor, usually a mobile PC or similar, and are updated within seconds or tenths of a second

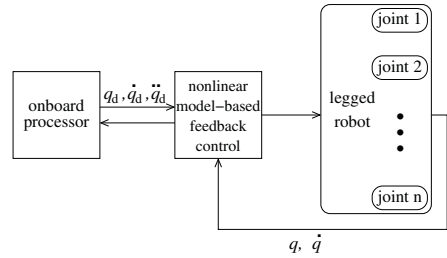


Fig. 5. Structure of a centralized, nonlinear model-based feedback control scheme: Its implementation requires the solution of the full nonlinear dynamic model described in Sect. 2 in real-time. Thus, strict requirements are imposed on the computational power and on the efficient coding of the dynamic equations. The reference trajectories are updated by an onboard processor (mobile PC) and are updated within seconds or tenths of a second for each new step while considering constraints and performance specifications

trajectory following control. Reference trajectories for the body posture, ZMP, or foot flight paths are developed off-line (e.g. through extensive simulations) and implemented on the bipedal robot using standard controllers such as PID to follow the reference trajectories which have been transformed to desired position (and velocity) information for each of the leg and foot joints (Fig. 4). This control strategy cannot easily nor automatically be adapted to a changing environment and can only handle relatively small changes to the reference data. However, it can be realized using decoupled, decentralized conventional control strategies in each of the joint motors. This strategy has been applied, e.g., to the Honda humanoid robot [18], the Humanoid H6 [27], [20], or [37] for a quadruped.

Feedback linearization techniques (computed torque) are also based on trajectory tracking techniques yet it takes full advantage of a nonlinear dynamical model to arrive at asymptotically stable closed-loop controllers. In contrast to simpler trajectory tracking schemes, these controllers are not decentralized nor decoupled. An example of this type of implementation may be found with Johnnie at the TU Munich [10].

In order to meet the challenge of producing fast and stable motions for bipedal and quadrupedal robots that can quickly adapt to a changing environment, nonlinear, model-based feedback control methods must be developed which can generate completely new motion trajectories through adaptation within a few seconds and ensure stability within milliseconds (Fig. 5). To achieve this goal, fast and robust modeling and simulation methods for legged robot dynamics are needed. Contributions have been described in this paper. Furthermore, a more centralized control scheme is needed. Decentralized joint controllers with standard control schemes, as provided with the often used servos, cannot satisfy these requirements.

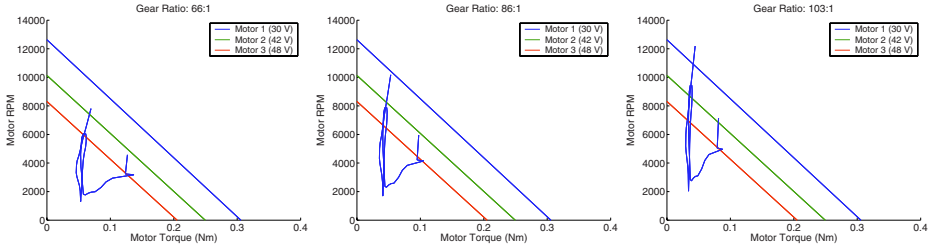


Fig. 6. Motor torque vs. rpm from an 18 kg biped with different motor/gear combinations

6 Robot Design and Dynamics of Legged Locomotion

To achieve optimal motion performance of an autonomous legged robot, especially a humanoid robot, a full dynamical study should ideally be made already in the design phase of the robot. The selection of motors and gears for the hip, knee or foot joints of a humanoid must be based on the expected applied force at each joint if the robot is walking or running while further considering the onboard energy supply and other hardware. These forces depend not only on the geometry of the robot links and joints but also on the distribution of masses in each part of the robot's body. The faster the robot moves, the stronger the motors and gears that are required. However, stronger motors and gears are also heavier and require more electrical power and, thus, more and heavier batteries. The heavier weight, though, will counteract the ability of fast walking. Thus, the design of a fast walking humanoid must find a good compromise between the different, counteracting objectives!

A design study was performed for the prototype of a fast walking humanoid (Fig. 2) using detailed numerical investigations with a nonlinear dynamical model. Numerical optimizations of *Energy Performance 1* in combination with maximum input power constraints were used to determine the minimum energy needed while moving at walking motions with speeds of up to 1.8 km/h. This preliminary analysis served to identify the most suitable class of motors. The final selection was based on graphing the torque-rpm workspace of interest for the respective joints during locomotion for a selection of different gear ratios and motors with different voltage ratings in combination with each motor's maximum operational characteristic line. The example displayed in Fig. 6 led to the choice of 42 V motors with 66:1 gear ratios. Minimum power requirements is a vital property for rapid locomotion and its autonomous functionality.

Ongoing joint work with the Control Systems Group of M. Buss at the Technische Universität Berlin is directed towards the completion of the construction, controller design, and remaining components such that this new humanoid robot may be presented in the 80 cm humanoid league at RoboCup.

7 Conclusion and Extensions

In this paper, the modeling, simulation and optimization of nonlinear dynamics and its role in the development and control of bipedal and quadrupedal robots is

investigated. A discussion is provided explaining the choice of robotic dynamics algorithms that are well-suited to legged systems together with efficient reduced dynamics algorithms to be used for increased numerical stability. A powerful and efficient numerical optimization framework is also presented which has been thoroughly tested in previous work in optimal gait planning. Several performance criteria have been presented which serve to either optimize energy or stability in legged systems. Much of this work has been geared towards the demanding setting of RoboCup where many external factors influence the robot's movement in a fast-changing dynamic environment. A minimax performance stability criteria is used for generating maximally stable quadruped gaits. The investigated dynamic stability criterion is well-suited to a changing environment and on-line stability assessment for closed-loop control design. The results must then be combined with trajectory tracking controllers which may additionally incorporate the stability index. At other times energy concerns are equally important such as in autonomous humanoid biped design. Efficient multibody algorithms combined with powerful numerical optimal control software solve energy-based performance criteria to aid in the humanoid construction design.

Acknowledgement

The authors thankfully acknowledge the information and help in using the Sony quadrupeds provided by Sony Corporation and its Open-R Support Team for this research.

References

1. Alexander, R.: The Gaits of Bipedal and Quadrupedal Animals. *International Journal of Robotics Research* **3**(2) (1984) 49–59
2. Betts, J.T.: Survey of numerical methods for trajectory optimization. *AIAA J. Guidance, Control, and Dynamics* **21**(2) (1998) 193–207
3. Buss, M., Glocker, M., Hardt, M., von Stryk, O., Bulirsch, R. Schmidt, G.: *Non-linear Hybrid Dynamical Systems: Modeling, Optimal Control, and Applications*. Submitted to *Lectures in Computer Science* (2002)
4. Channon, P.H.; Pham, D.T.; Hopkins, S.H.: Variational Approach to the Optimization of Gait for a Bipedal Robot. *Journal of Mechanical Engineering Science* **210** (1996) 177–186
5. Chevallereau, C.; Aoustin, Y.: Optimal reference trajectories for walking and running of a biped robot. *Robotica* **19**(5) (2001) 557–569
6. Chow, C.K.; Jacobson, D.H.: Studies of human locomotion via optimal programming. *Mathematical Biosciences* **10** (1971) 239–306
7. Denk, J.; Schmidt, G.: Walking primitive synthesis for an anthropomorphic biped using optimal control techniques. *CLAWAR: Int. Conf. on Climbing and Walking Robots* (2001)
8. Featherstone, R.: *Robot Dynamics Algorithms*. Kluwer Academic Publishers (1987)
9. Featherstone, R.; Orin, D.: *Robot Dynamics: Equations and Algorithms*. *IEEE Int. Conf. on Robotics and Automation* (2000) 826–34

10. Gienger, M.; Löffler, K.; Pfeiffer, F.: Towards the Design of a Biped Jogging Robot. *IEEE Int. Conf. on Robotics and Automation* (2001) 4140–45
11. Gill, P.E.; Murray, W.; Saunders, M.A.: *User's Guide for SNOPT 5.3: a Fortran Package for Large-Scale Nonlinear Programming*, Math. Dept., Univ. of California, San Diego (1997)
12. Goswami, A.: Postural Stability of Biped Robots and the Foot-Rotation Indicator (FRI) Point. *International Journal of Robotics Research* **18**(6) (1999) 523–533
13. Gregorio, P.; Ahmadi, M.; Buehler, M.: Design, Control, and Energetics of an Electrically Actuated Legged Robot. *IEEE Systems, Man and Cybernetics, Part B* **27**(4) (1997) 626–634
14. Grizzle, J.W.; Abba, G.; Plestan, F.: Asymptotically stable walking for biped robots: Analysis via systems with impulse effects. *IEEE Trans. Automatic Control* **46** (2001) 51–64
15. M. Hardt, *Multibody Dynamical Algorithms, Numerical Optimal Control, with Detailed Studies in the Control of Jet Engine Compressors and Biped Walking*. Ph.D. Thesis, Electrical Engineering, University of California San Diego, U.S.A. (1999)
16. Hardt, M.; Helton, J.W.; Kreutz-Delgado, K.: Optimal Biped Walking with a Complete Dynamical Model. *IEEE Conference on Decision and Control* (1999) 2999–3004
17. Hardt, M.; von Stryk, O.: Towards Optimal Hybrid Control Solutions for Gait Patterns of a Quadruped. *CLAWAR: Int. Conf. on Climbing and Walking Robots* (2000) 385–392
18. Hirai, K.; Hirose, M.; Haikawa, Y.; Takenaka, T.: The Development of Honda Humanoid Robot. *IEEE Int. Conf. on Robotics and Automation* (1998) 1321–26
19. Hu, J.; Pratt, G.: Nonlinear Switching Control of Bipedal Walking Robots with Provable Stability. *Humanoid conference, Boston, U.S.A.* (2000)
20. Huang, Q.; Yokoi, K.; Kajita, S.; Kaneko, K.; Arai, H.; Koyachi, N.; Tanie, K.: Planning Walking Patterns for a Biped Robot. *IEEE Trans. Robotics and Automation* **116** (1994) 30–36
21. Hurmuzlu, Y.; Basdogan, C.: On the Measurement of Dynamic Stability of Human Locomotion. *ASME Journal Biomechanical Engineering* **116** (1994) 30–36
22. Kajita, S.; Tanie, K.: Experimental study of biped dynamic walking. *IEEE Control Systems Magazine* **16**(1) (1996) 13–19
23. Kimura, H.; Shimoyama, I.; Miura, H.: Dynamics in the Dynamic Walk of a Quadruped Robot. *Advanced Robotics* **4**(3) (1990) 283–301
24. Koo, T.W.; Yoon, Y.S.: Dynamic instant gait stability measure for quadruped walking robot. *Robotica* **17** (1999) 59–71
25. McMillan, S.; Orin, D.E.: Efficient Computation of Articulated-Body Inertias Using Successive Axial Screws. *IEEE Trans. on Robotics and Automation* **11**(4) (1995) 606–11
26. Mombaur, K.D.; Bock, H.G.; Schlöder, J.P.; Longman, R.W.: Human-like actuated walking that is asymptotically stable without feedback. *IEEE Int. Conf. on Robotics and Automation* (2001) 4128–33
27. Nishiwaki, K.; Sugihara, T.; Kagami, S.; Inaba, M.; Inoue, H.: Online Mixture and Connection of Basic Motions for Humanoid Walking Control by Footprint Specification. *IEEE Int. Conf. on Robotics and Automation* (2001) 4110–15
28. Otter, M.; Elmqvist, H.; Cellier, F.E.: Modeling of Multibody Systems with the Object-Oriented Modeling Language Dymola. *Nonlinear Dynamics* **9** (1996) 91–112

29. Pai, D.K.; Ascher, U.M.; Kry, P.G.: Forward Dynamics Algorithms for Multibody Chains and Contact. *IEEE Int. Conf. on Robotics and Automation* (2000) 857–63
30. Pfeiffer, F.; Glocker, C.: *Multibody Dynamics with Unilateral Contacts*. Wiley Series Nonlinear Science, New York (1996)
31. Rodriguez, G.; Kreutz-Delgado, K.; Jain, A.: A Spatial Operator Algebra for Manipulator Modeling and Control. *International Journal of Robotics Research* **40** (1991) 21–50
32. von Stryk, O.: DIRCOL: A direct collocation method for the numerical solution of optimal control problems. Technische Universität Darmstadt, World Wide Web: <http://www.sim.informatik.tu-darmstadt.de/sw/dircol> (2001)
33. von Stryk, O.; Glocker, M.: Numerical mixed-integer optimal control and motorized travelling salesmen problems. *APII-JESA – European Journal of Control* **35**(4) (2001) 519–533
34. Yamamoto, Y.; Fujita, M.; de Lasa, M.; Talebi, S.; Jewell, D.; Playter, R.; Raibert, M.: Development of dynamic locomotion for the entertainment robot – teaching a new dog old tricks. *CLAWAR: Int. Conf. on Climbing and Walking Robots* (2001) 695–702
35. Vukobratović, M.; Borovac, B.; Surla, D.; Stokić, D.: *Biped Locomotion. Dynamics, Stability, Control, and Application*. Springer-Verlag, Berlin (1990)
36. Walker, M.W.; Orin, D.E.: Efficient Dynamic Computer Simulation of Robotic Mechanisms. *Trans. ASME Journal of Dynamic Systems, Measurement, & Control* **104** (1982) 205–211
37. Yoneda, K.; Iiyama, H.; Hirose, S.: Intermittent trot gait of a quadruped walking machine dynamic stability control of an omnidirectional walk. *IEEE Int. Conf. on Robotics and Automation* (1996) 3002–7